of the active species can be explored by *operando* APXPS measurements. This crucial information serves as a foundation for designing and optimizing electrocatalysts with better performance. (Reported by Chia-Hsin Wang)

This report features the work of Chia-Hsin Wang and his collaborators published in ChemCatChem ***15****, e202300359 (2023), and the work of Yu-Hsu Chang and his collaborators published in ACS Catal.* ***13****, 13434 (2023).*

TLS 24A1 XPS, UPS, XAS, APXPS

- XPS, UPS, Ambient Pressure XPS
- Materials Science

References

1. C.-C. Yang, M.-H. Tsai, Z.-R. Yang, Y.-C. Tseng, C.-H. Wang, ChemCatChem **15**, e202300359 (2023).
2. P. Patta, Y.-Y. Chen, M. Natesan, C.-L. Sung, C.-C. Yang, C.-H. Wang, T. Fujigaya, Y.-H. Chang, ACS Catal. **13**, 13434 (2023).

Operando X-ray Absorption Spectroscopic Studies within a Flow Cell for Carbon Dioxide Reduction Reaction

Utilizing a flow cell can significantly boost the catalytic activities of the carbon dioxide reduction reaction. Employing an operando flow cell that mimics the catalytic environment allows for the investigation of the chemical and structural evolution in highly efficient catalysts.

The escalating concentration of atmospheric CO_2 has led to severe global warming and climate change. The electrochemical CO_2 reduction reaction (CO_2RR) is regarded as a promising avenue for both alleviating CO_2 levels while concurrently yielding valuable products such as ethylene and ethanol. The utilization of a flow cell is pivotal for establishing an industrially viable CO_2RR process, substantially amplifying catalytic performance, especially in terms of catalytic current density, with enhancements ranging from ten to a hundredfold. This highlights the distinctive catalytic environment and behavior characteristics of a flow cell. To unveil the authentic properties of a catalyst within a flow cell, Sung-Fu Hung (National Yang Ming Chiao Tung University) and his team meticulously devised a flow cell tailored for *operando* X-ray absorption spectroscopy (XAS) during CO_2RR, accurately replicating the electrocatalytic conditions.[1] This innovative technique allows assessment of the authentic forms of the catalysts in diverse catalyst systems and facilitates the development of synthetic strategies aimed at achieving high catalytic activity.

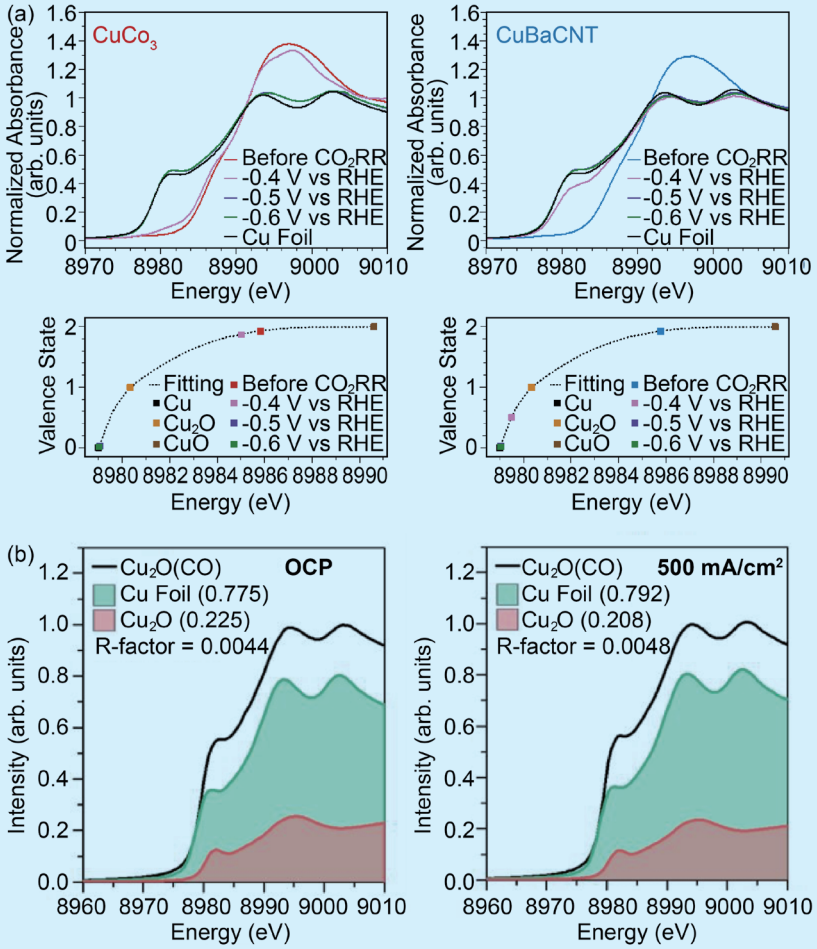

Fig. 1: (a) *Operando* XANES and valence-state analyses for $CuCO_3$ and CuBaCNT during CO_2RR. (b) *Operando* XANES and linear combination fitting for $Cu_2O(CO)$ at open-circuit potential (OCP) and 500 mA cm^{-2} during CO_2RR. [Reproduced from Refs. 2 and 3]

A nanocomposite composed of carbon nanotubes adorned with copper and barium (CuBaCNT) was designed to elevate catalyst conductivity, alter the 3d orbitals of Cu (validated through 1s3p resonant inelastic X-ray scattering at **SP 12U1**), and augment selectivity and current density.[2] CuBaCNT demonstrated a Faradaic efficiency of 70.9% and a partial current density of 354.6 mA cm^{-2} for C_2 products at 500 mA cm^{-2}. This outperformed $CuCO_3$, which exhibited a Faradaic efficiency of 67.8% and a partial current density of 203.3 mA cm^{-2} for C_2 products at 300 mA cm^{-2}. *Operando* X-ray absorption near edge structure (XANES) experiments conducted at the **TLS 17C1** unveiled the swift reduction of Cu in CuBaCNT during CO_2RR (**Fig. 1(a)**). The analysis of valence states that employs the zero crossing of the second derivative of the spectra suggested a valence state from +1.9 to +0.5 at –0.4 V vs RHE, which transitions into a metallic state at a more negative voltage. This transformation was attributed to the incorporation of carbon nanotubes, which improved overall conductivity and established a conductive network facilitating efficient electron transport to the electrocatalysts. Consequently, the authentic form of the catalyst during CO_2RR appeared to be metallic Cu rather than $CuCO_3$, which is the original composition of CuBaCNT.

In addition to enhancing catalyst conductivity, establishing a stable interface between Cu^0 and Cu^+ within the catalyst represents a promising strategy for elevating catalytic activity. A method for achieving this stable interface involved the creation of rich nanograin boundaries through the thermal reduction of Cu_2O nanocubes in a carbon monoxide (CO) atmosphere, referred to as $Cu_2O(CO)$.[3] This catalyst demonstrated a Faradaic efficiency of 77.4% and a partial current density for C_{2+} products at 387.0 mA cm^{-2} at 500 mA cm^{-2}, which surpass those of bare Cu_2O, which exhibited a Faradaic efficiency of 61.5% and a partial current density of 184.5 mA cm^{-2} for C_{2+} products at 300 mA cm^{-2}. *Operando* XANES experiments conducted at the **SP 12B1** were employed to validate the impact of nanograin boundaries on Cu^0/Cu^+ interfacial sites within the $Cu_2O(CO)$ electrocatalyst during CO_2RR. The linear recombination fitting results of XANES in **Fig. 1(b)** revealed that $Cu_2O(CO)$ consisted of 77.5% metallic Cu and 22.5% Cu_2O before CO_2RR, while over 20% Cu_2O still remained during CO_2RR. This observation indicated that the considerable presence of nanograin boundaries in the $Cu_2O(CO)$ electrocatalyst effectively impeded the reduction of Cu to a metallic state, thereby enhancing catalytic stability.

Both particle size and coordination play crucial roles in determining the selectivity of CO_2RR. A Cu catalyst with low coordination can effectively limit C–C coupling, promoting CO_2 methanation. A recent design approach utilized carbon nanoparticles (CNPs) and multi-dentate coordination using ethylenediaminetetraacetic acid (EDTA) to control the size of Cu clusters derived from the copper phthalocyanine (CuPc) precursor, showcasing its performance in acidic CO_2RR for methane production.[4] Constrained by EDTA, EDTA/CuPc/CNP achieved a Faradaic efficiency of 71% and a partial current density of 71 mA cm^{-2} at 100 mA cm^{-2} toward CH_4. In contrast, EDTA/CuPc exhibited a lower Faradaic efficiency toward CH_4 at 48.9%, coupled with higher C_2H_4 production. This emphasizes

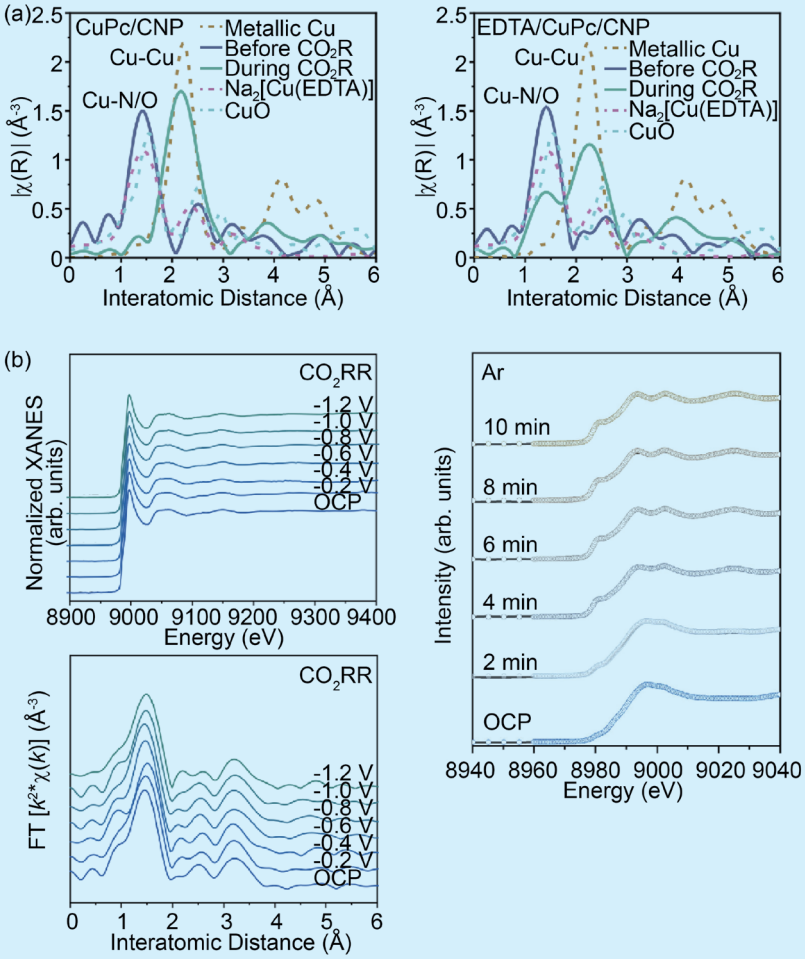

Fig. 2: (a) *Operando* EXAFS spectra for CuPc/CNP and EDTA/CuPc/CNP during CO_2RR. (b) *Operando* X-ray absorption spectroscopy during CO_2RR and under an Ar atmosphere (200 mA cm^{-2}). [Reproduced from Refs. 4 and 5]

the multi-dentate chelating effect of EDTA for enhancing CH_4 selectivity. *Operando* extended X-ray absorption fine structure (EXAFS) experiments conducted at the **TLS 17C1** provided insights into the CuPc/CNP and EDTA/CuPc/CNP catalysts. In **Fig. 2(a)**, the results show that the peak corresponding to the Cu–Cu metallic bond increased, while the Cu–N/O peak significantly decreased during CO_2RR due to the reduction of Cu(II) and agglomeration. With EDTA decoration, the peaks corresponding to the Cu–Cu and Cu–N/O bonds showed slight increases and decreases, respectively. This indicates that EDTA, acting as a chelating agent, restrains the Cu ions, maintaining their structure and generating only small Cu clusters. The *operando* experiments demonstrated the chelating effect of EDTA on Cu ions, which influenced the chemical and physical properties of Cu species in the EDTA/CuPc/CNP during CO_2RR, promoted CH_4 selectivity.

Metal–organic frameworks (MOFs) are distinguished by numerous coordinative void spaces and high surface areas, making them potential candidates for CO_2RR if a robust structure can be achieved. A copper-based MOF catalyst, Cu(OH)BTA (Cu atoms coordinating with deprotonated 1H-BTA and transversely connecting through hydroxyl groups), has been developed for CO_2RR.[5] This catalyst achieved a Faradaic efficiency of 73% and a partial current density for C_{2+} products of 365 mA cm^{-2} at 500 mA cm^{-2}. To investigate the Cu active sites of Cu(OH)BTA during CO_2RR, *operando* XAS experiments were conducted at the **TPS 44A** (**Fig. 2(b)**). *Operando* XANES spectra identified that the Cu oxidation state remained unaltered throughout the entire potential range of CO_2RR, while there was no discernible peak corresponding to the Cu–Cu metallic bond in the EXAFS spectra. This suggests that Cu maintained atomic dispersion in a coordinative manner throughout the CO_2RR. In contrast, the XANES spectra of Cu(OH)BTA exhibited characteristics of metallic Cu within 10 min at 200 mA cm^{-2} under an Ar atmosphere. This underscores the robust nature of Cu(OH)BTA during CO_2RR.

In summary, the innovation of a flow cell for CO_2RR represents a significant advancement that greatly enhances catalytic activity. Diverse catalyst designs can further regulate the selectivity and partial current density of the end product in CO_2RR. This report highlights various design strategies, including enhancing conductivity with carbon nanotubes, stabilizing the Cu^0/Cu^+ interface through nanograin boundaries, restricting Cu cluster size by incorporating EDTA and CNPs, and developing a robust MOFs catalyst. All these approaches demonstrated a notable improvement in selectivity and catalytic current density. The high current density observed in a highly reductive environment allows for the development of *operando* X-ray absorption spectroscopy within a flow cell, which replicates the electrocatalytic environment, providing an accurate reflection of the authentic catalyst form. This approach helps elucidate the proper mechanisms for achieving highly efficient CO_2RR. (Reported by Sung-Fu Hung, National Yang Ming Chiao Tung University)

This report features the works of Sung-Fu Hung and his collaborators published in J. Mater. Chem. A ***11****, 13217 (2023), ACS Nano* ***17****, 12884 (2023), Nat. Commun.* ***14****, 3314 (2023), and Nat. Commun.* ***14****, 474 (2023).*

TPS 44A Quick-scanning X-ray Absorption Spectroscopy
TLS 17C1 EXAFS
SP 12B1 Materials X-ray Study
SP 12U1 Inelastic X-ray Scattering

- XAS, RIXS
- Materials Science, Chemistry

References

1. S. F. Hung, F.-Y. Wu, Y.-H. Lu, T.-J. Lee, H.-J. Tsai, P.-H. Chen, Z.-Y. Lin, G.-L. Chen, W.-Y. Huang, W.-J. Zeng, Catal. Sci. Technol. **12**, 2739 (2022).
2. F.-Y. Wu, H.-J. Tsai, T.-J. Lee, Z.-Y. Lin, K.-S. Peng, P.-H. Chen, N. Hiraoka, Y.-F. Liao, C.-W. Hu, S.-H. Hsu, Y.-R. Lu, S.-F. Hung, J. Mater. Chem. A **11**, 13217 (2023).
3. Q. Wu, R. Du, P. Wang, G. I.N. Waterhouse, J. Li, Y. Qiu, K. Yan, Y. Zhao, W.-W. Zhao, H.-R. Tsai, M.-C. Chen, S.-F. Hung, X. Wang, G. Chen, ACS Nano **17**, 12884 (2023).
4. M. Fan, R. K. Miao, P. Ou, Y. Xu, Z.-Y. Lin, T.-J. Lee, S.-F. Hung, K. Xie, J. E. Huang, W. Ni, J. Li, Y. Zhao, A. Ozden, C. P. O'Brien, Y. Chen, Y. C. Xiao, S. Liu, J. Wicks, X. Wang, J. Abed, E. Shirzadi, E. H. Sargent, D. Sinton, Nat. Commun. **14**, 3314 (2023).
5. Y. Liang, J. Zhao, Y. Yang, S.-F. Hung, J. Li, S. Zhang, Y. Zhao, A. Zhang, C. Wang, D. Appadoo, L. Zhang, Z. Geng, F. Li, J. Zeng, Nat. Commun. **14**, 474 (2023).

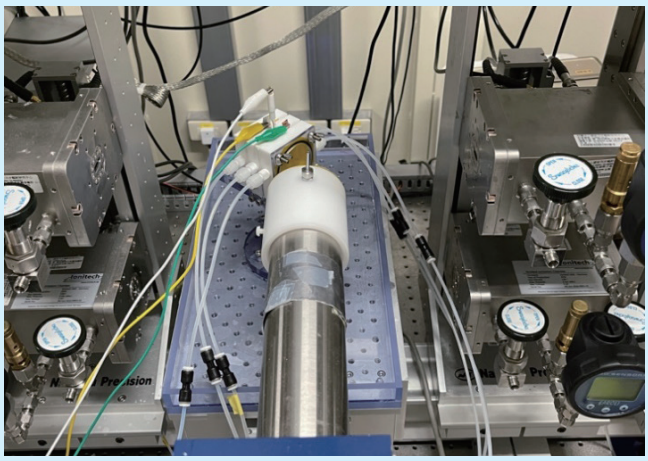

TPS 44A setup of an *Operando* flow cell for X-ray absorption spectroscopy